UNSYMMETRIC WRINKLING OF CIRCULAR PLATES*

BY

L. S. CHEO (*The William Paterson College of New Jersey*)

AND

EDWARD L. REISS (*Courant Institute of Mathematical Sciences*)

Abstract. The branching of unsymmetric equilibrium states from axisymmetric equilibrium states for clamped circular plates subjected to a uniform edge thrust and a uniform lateral pressure is analyzed in this paper. The branching process is called wrinkling and the loads at which branching occurs are called wrinkling loads. The nonlinear von Kármán plate theory is employed. The wrinkling loads are determined by solving numerically the eigenvalue problem obtained by linearizing about a symmetric equilibrium state. The post-wrinkling behavior is studied by a perturbation expansion in the neighborhood of the wrinkling loads.

1. Introduction. The nonlinear axisymmetric bending and buckling of circular plates have been investigated extensively for a variety of boundary and loading conditions. In this paper we shall study axially unsymmetric equilibrium states of clamped circular plates that are deformed by uniform axisymmetric surface and edge loads. We employ the nonlinear von Kármán plate theory [1]. This yields a boundary-value problem, which we call Problem B, for a coupled system of two fourth order partial differential equations.

In particular, we shall seek unsymmetric states that branch from non-trivial axisymmetric equilibrium states. We refer to this as wrinkling (cf. [2]) and the branch points, i.e. the loads at which branching is initiated, as the wrinkling loads. To determine the wrinkling loads, we linearize unsymmetric solutions of Problem B about axisymmetric solutions. The eigenvalues of the resulting eigenvalue problem are wrinkling loads. Since the coefficients in the differential equations of the eigenvalue problem are functions of the axisymmetric solutions, the eigenvalue parameter appears nonlinearly.

We solve the eigenvalue problem numerically by a difference method that is essentially equivalent to a procedure used by Huang [3] in a related study of the buckling of spherical caps. The coefficients in the differential equations of the eigenvalue problem are approximated by solving numerically the axisymmetric Problem B by the shooting method described in [4]. We use a formal perturbation expansion to analyze the unsymmetric states near the wrinkling loads. The resulting linear problems are solved numerically by the shooting and parallel shooting methods [4].

* Received March 17, 1972. The research reported in this paper was supported by the National Science Foundation, Grant GP-27223 and the Office of Naval Research, Contract N000 14-67-A-0467-0006. It is based in part on a thesis submitted by L. S. Cheo to New York University in partial fulfillment of the requirements for the degree of Doctor of Philosophy. The authors appreciate the helpful suggestions of Dr. Louis Bauer.

If the plate is deformed by a uniform edge thrust only and the axisymmetric state is a buckled equilibrium state, then the wrinkling is also called secondary buckling. Friedrichs and Stoker [5] conjectured that secondary buckling may occur for simply supported circular plates. Morozov [6] showed that for sufficiently large edge thrusts, unsymmetric equilibrium states exist for the simply supported circular plate. In addition, these unsymmetric states have less potential energy than all axisymmetric states for the same value of the edge thrust. However, Morozov did not show that secondary buckling occurs. Yanowitch [2] previously obtained results related to [6] for other boundary and loading conditions. In this paper we obtain approximations of secondary buckling loads for the clamped circular plate.

In the pure bending problem the edge thrust vanishes and the plate is deformed only by the uniform surface pressure. The wrinkling loads are then the values of the pressure at which unsymmetric states bifurcate from the unique axisymmetric state.

In the combined loading problem, the edge thrust and the pressure do not vanish. We analyze this problem by keeping the thrust fixed and then increasing the pressure from zero until wrinkling occurs. The axisymmetric state is the one obtained by this loading process. If the thrust exceeds the lowest buckling load of the plate and the pressure is zero, then the axisymmetric state is the lowest buckled state. The pressure is then applied in the "direction that the plate is buckled;" i.e., the pressure acts to increase the amplitude of the buckled state.

2. Formulation. The radius and thickness of the circular plate are denoted by R and t. The applied axisymmetric loads are a uniform radial edge stress T and a uniform surface pressure p. We employ a polar coordinate system r, θ with respect to the plate's center. The displacement normal to the midplane, and the midplane (membrane) stresses are denoted respectively by $W^*(r, \theta)$, $\sigma_r(r, \theta)$, $\sigma_\theta(r, \theta)$ and $\sigma_{r\theta}(r, \theta)$. (The subscripts on σ indicate components of stress. Subscripts r, θ or x on any other variable indicate partial differentiation.) The Airy stress function $F^*(r, \theta)$ is defined by

$$\sigma_r = r^{-2}(rF^*_r + F^*_{\theta\theta}), \qquad \sigma_\theta = F^*_{rr}, \qquad \sigma_{r\theta} = -(r^{-1}F^*_\theta)_r . \tag{2.1}$$

We define dimensionless variables and parameters by

$$x \equiv r/R, \qquad W(x, \theta) \equiv CW^*(r, \theta)/t, \qquad F(x, \theta) \equiv (C^2/Et^2)F^*(r, \theta),$$
$$\lambda \equiv -C^2(T/E)(R/t)^2, \qquad P \equiv C^3(p/E)(R/t)^4, \qquad C \equiv [12(1 - \nu^2)]^{1/2}. \tag{2.2}$$

Here E is Young's modulus and ν is Poisson's ratio. The edge thrust parameter λ is positive when $T < 0$, i.e. when the thrust is compressive. The boundary value problem of the von Kármán plate theory, which we call Problem B, is given by

$$\begin{aligned} \Delta^2 F &= -(1/2)[W, W], \\ \Delta^2 W &= P + [F, W], \end{aligned} \quad \text{for} \quad x < 1, 0 \le \theta \le 2\pi, \tag{2.3a}$$

$$W(1, \theta) = W_x(1, \theta) = 0, \tag{2.3b}$$

$$F(1, \theta) = 0; \qquad F_x(1, \theta) = -\lambda, \qquad 0 \le \theta \le 2\pi. \tag{2.3c}$$

Here the Laplacian Δ and the nonlinear operator $[g, h]$ are defined for any two functions $g(x, \theta)$ and $h(x, \theta)$ by

$$\Delta g \equiv g_{xx} + (1/x)g_x + (1/x^2)g_{\theta\theta} ,$$
$$[g, h] \equiv \frac{1}{x}\left\{g_{xx}\left[h_x + \frac{1}{x}h_{\theta\theta}\right] + h_{xx}\left[g_x + \frac{1}{x}g_{\theta\theta}\right] - 2x\left[\frac{h_\theta}{x}\right]_x\left[\frac{g_\theta}{x}\right]_x\right\}. \tag{2.4}$$

The boundary conditions (2.3b) imply that the edge is clamped and the conditions (2.3c) imply, using (2.1) and (2.2), that $\sigma_r(R, \theta) = T$ and $\sigma_{r\theta}(R, \theta) = 0$. If $P \neq 0$ ($P = 0$) and $\lambda = 0$ ($\lambda > 0$), then we refer to Problem B as a pure bending (buckling) problem. If $P \neq 0$ and $\lambda \neq 0$, then Problem B is the combined loading problem.

We denote any axisymmetric solution of Problem B by $\{W_0(x), F_0(x)\}$. We define new dependent variables $\alpha(x)$ and $\gamma(x)$ by

$$\alpha(x) \equiv W_0'(x), \quad \gamma(x) \equiv F_0'(x), \tag{2.5}$$

where a prime denotes differentiation with respect to x. Then Problem B for axisymmetric solutions is reduced to [7]

$$\begin{aligned} L\gamma &= -(1/2)\alpha^2, \qquad L\alpha = \alpha\gamma + (P/2)x^2, \\ \alpha(0) &= \gamma(0) = 0, \qquad \alpha(1) = 0, \qquad \gamma(1) = -\lambda, \end{aligned} \tag{2.6}$$

where the differential operator L is defined by

$$Lv(x) \equiv x[(xv)'/x]'. \tag{2.7}$$

We refer to the boundary-value problem (2.6) as Problem S. If $\lambda \leq 0$ then Problem S has a unique solution [8]. If λ is positive and sufficiently large then Problem S may have non-unique solutions.

We seek unsymmetric solutions of Problem B which branch from a solution of Problem S. For the pure buckling problem this corresponds to studying secondary buckling from a buckled axisymmetric state. The physical mechanism that initiates wrinkling is suggested by the following properties of the solutions of Problem S (see, e.g., [5, 7]). We define a dimensionless, axisymmetric circumferential membrane stress $\tau(x)$ by

$$\tau(x) \equiv C^2(R/t)^2\sigma_\theta(r)/E. \tag{2.8}$$

In Fig. 1 we present graphs obtained from a numerical solution of Problem S with $P = 0$ [7]. As λ increases, a strip of large circumferential compressive stress develops adjacent to the edge of the plate. The "width" of the strip decreases and the compressive stress intensity increases as λ increases. Thus for sufficiently large λ the strip may buckle unsymmetrically like a ring, i.e. the plate may buckle about the axisymmetric buckled state by wrinkling near the edge into an unsymmetric state. Secondary buckling is related to von Kármán's concept of the ultimate load of rectangular plates buckled by an edge thrust [9]. The width of the strip is related to the "effective width" of rectangular plates.

In Figs. 2 and 3 we present graphs obtained from numerical solutions [7] of Problem S with $\lambda = 0$, $\lambda = 80$, respectively. Thus wrinkling may occur for sufficiently large P for the pure bending and the combined loading problems by the same mechanism as in the pure buckling problem.

3. The wrinkling loads. To determine the wrinkling loads we express unsymmetric

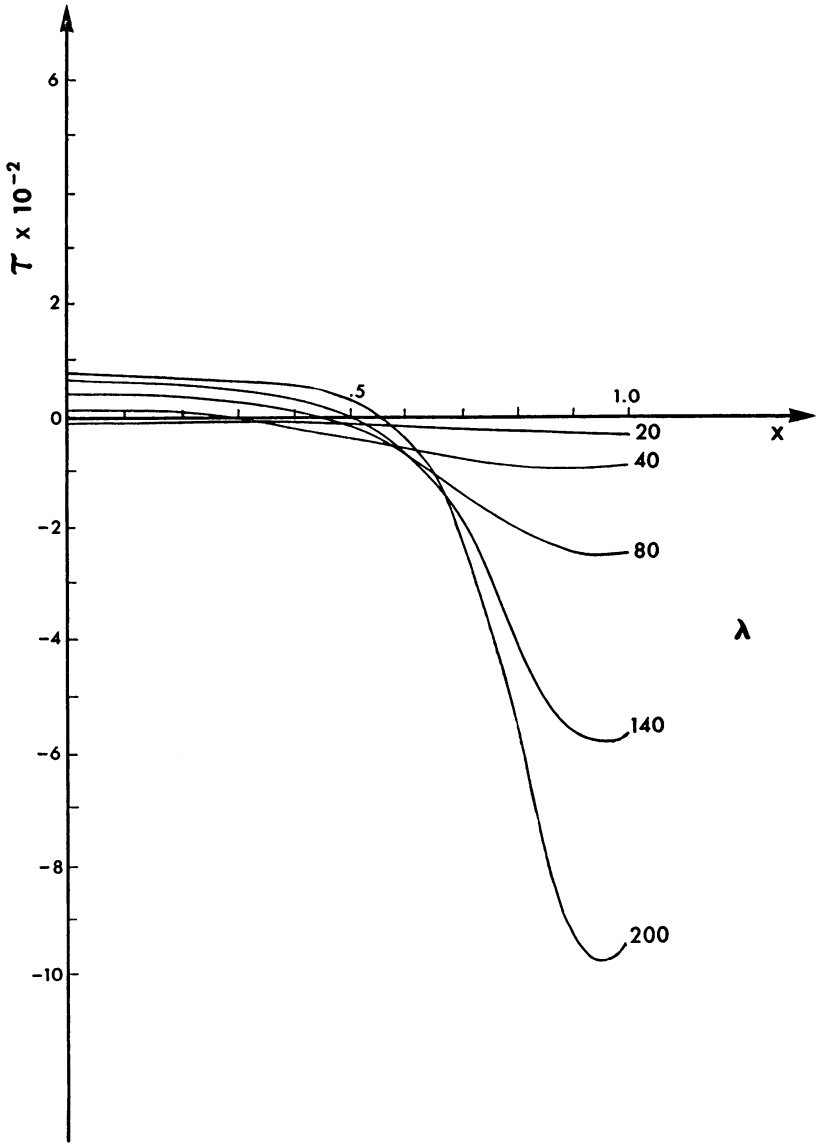

FIG. 1. The dimensionless axisymmetric circumferential membrane stress for the pure buckling problem, Problem S with $P = 0$, for an increasing sequence of values of λ. The solutions correspond to equilibrium states on the branch emanating from the lowest axisymmetric buckling load $\lambda = \lambda_1 \approx 14.7$.

solutions $\{W(x, \theta; P, \lambda), F(x, \theta; P, \lambda)\}$ of Problem B in the form

$$\begin{aligned} W(x, \theta; P, \lambda) &= W_0(x; P, \lambda) + \epsilon w(x, \theta; P, \lambda, \epsilon) \\ F(x, \theta; P, \lambda) &= F_0(x; P, \lambda) + \epsilon f(x, \theta; P, \lambda, \epsilon) \end{aligned} \tag{3.1}$$

where $\{W_0, F_0\}$ is a solution of Problem S and ϵ is a small parameter. We insert (3.1) into (2.3) and obtain

$$\begin{aligned} \Delta^2 f + [W_0, w] &= (-\epsilon/2)[w, w], \\ \Delta^2 w - [W_0, f] - [F_0, w] &= \epsilon[f, w], \\ w = w_x = f = f_x &= 0, \qquad x = 1. \end{aligned} \tag{3.2}$$

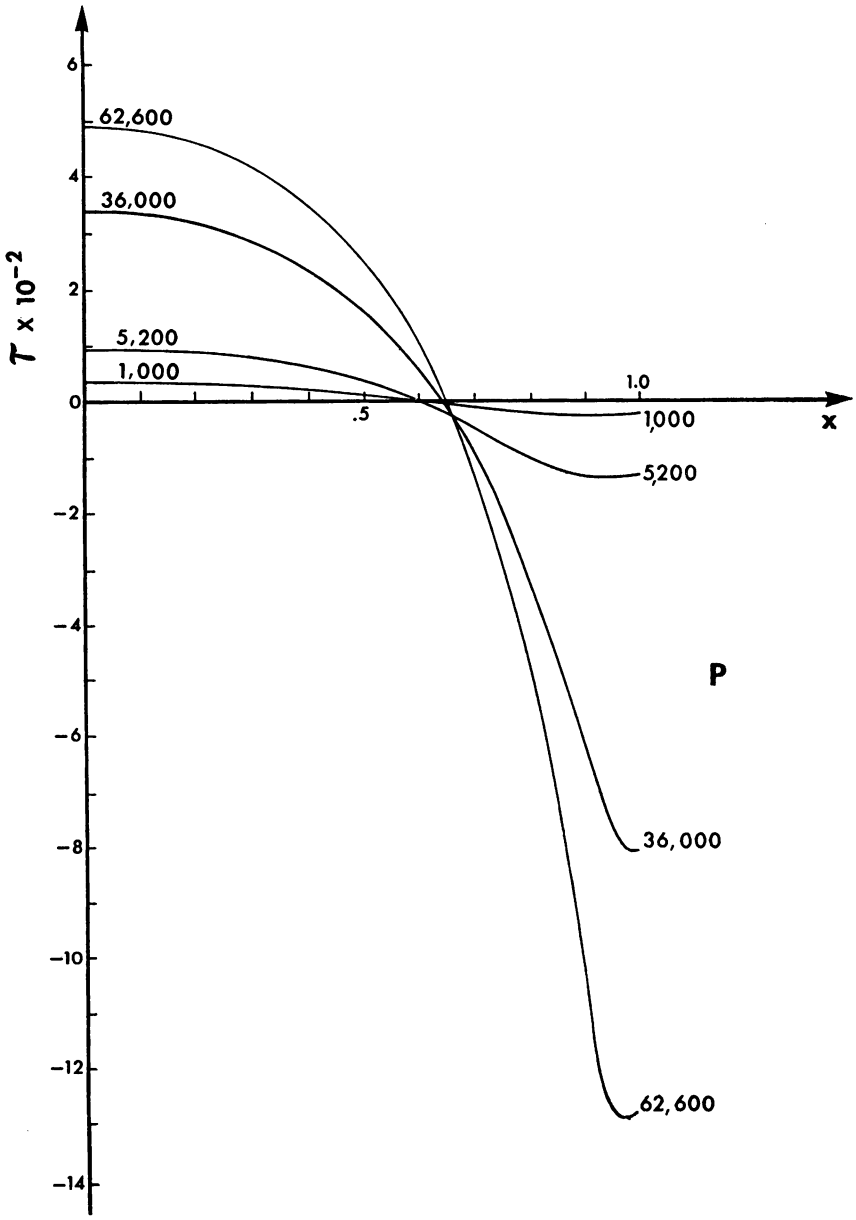

FIG. 2. The dimensionless, axisymmetric, circumferential membrane stress for the pure bending problem, Problem S with $\lambda = 0$, for an increasing sequence of values of P. A ring of large compressive stress develops near the boundary as P increases. The width of the ring decreases and the intensity of the stress increases as P increases. This indicates the possibility of wrinkling near the edge.

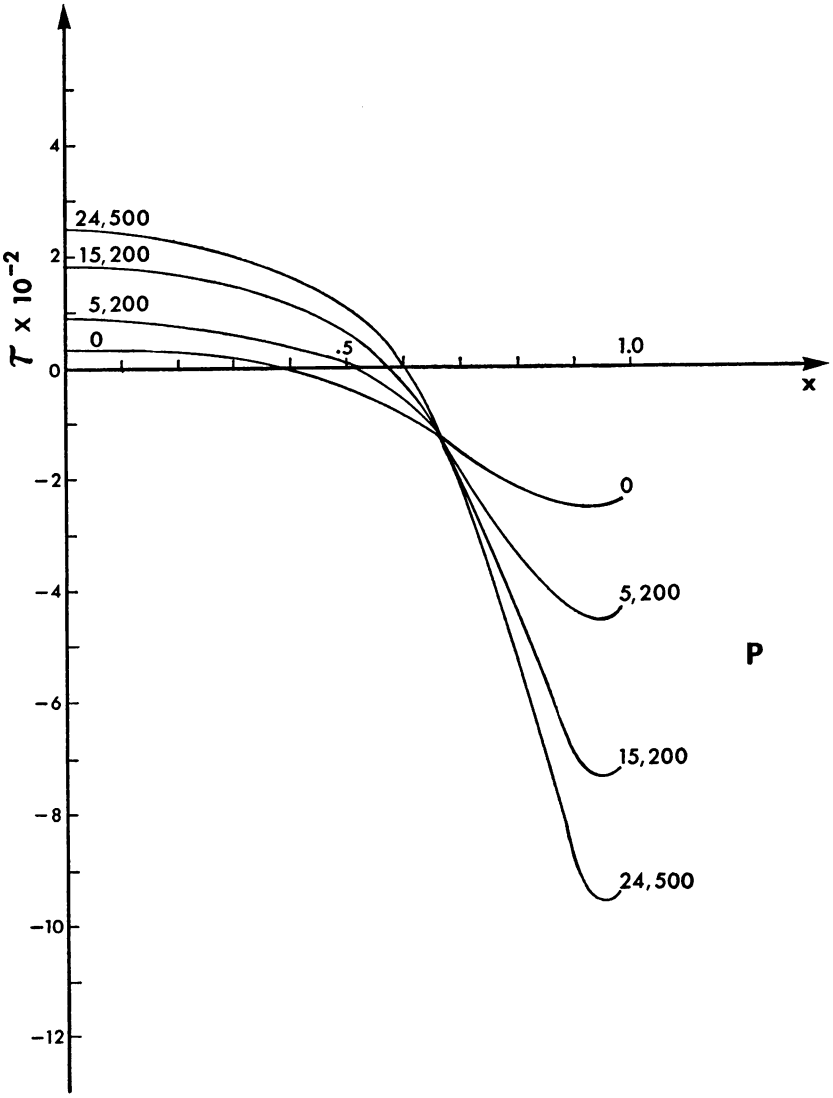

FIG. 3. $\tau(x)$ for Problem S with $\lambda = 80$ and an increasing sequence of values of P. For $P = 0$, the solution corresponds to an axisymmetric buckled state on the branch that bifurcates from $\lambda = \lambda_1$. The development of a compressive ring as P increases, and the consequent possibility of wrinkling, is evident from the graphs.

We linearize (3.2) by setting $\epsilon = 0$ in (3.2). This yields the eigenvalue problem

$$\begin{aligned} &\Delta^2 f^{(0)} + [W_0\,,\, w^{(0)}] = 0, \\ &\Delta^2 w^{(0)} - [W_0\,,\, f^{(0)}] - [F_0\,,\, w^{(0)}] = 0, \\ &w^{(0)} = w_x^{(0)} = f^{(0)} = f_x^{(0)} = 0, \qquad x = 1. \end{aligned} \tag{3.3}$$

where $w^{(0)} \equiv w(x, \theta; P, \lambda, 0)$, $f^{(0)} \equiv f(x, \theta; P, \lambda, 0)$.

For any pair of values of (P, λ), $w^{(0)} = f^{(0)} \equiv 0$ is a solution of (3.3). For the combined loading problem, we shall determine for fixed values of λ and a specific solution of Problem S, the eigenvalues $P = P_0(\lambda)$ of (3.3), i.e. the values of P for which (3.3) has nontrivial solutions. The eigenvalues are wrinkling loads. Since $\{W_0(x; P, \lambda), F_0(x; P, \lambda)\}$ is a solution of Problem S, the eigenvalue parameter appears nonlinearly in (3.3). For the pure buckling problem ($P = 0$) and a specific axisymmetric buckled state, we shall determine values of λ for which (3.3) has nontrivial solutions. Then λ is the eigenvalue parameter in (3.3). The eigenvalues are secondary buckling loads.

The eigenfunctions of (3.3) are separable. Without loss of generality they are given by *

$$\begin{aligned} f^{(0)} &= y_n(x; P, \lambda) \sin n\theta, \\ w^{(0)} &= z_n(x; P, \lambda) \sin n\theta \end{aligned} \tag{3.4}$$

for $n = 1, 2, \cdots$. Here $\{y_n, z_n\}$ satisfy

$$\begin{aligned} L_n^2 y_n + [W_0, z_n]^0 &= 0, \\ L_n^2 z_n - [W_0, y_n]^0 - [F_0, z_n]^0 &= 0, \end{aligned} \tag{3.5}$$

$$y_n = y_n' = z_n = z_n' = 0, \quad \text{for} \quad x = 1, \tag{3.6a}$$

where $[\Phi_0, h]^0$ and the differential operators L_n are defined by

$$L_n h(x) \equiv (1/x)(xh')' - (n^2/x^2)h, \qquad n = 1, 2, \cdots,$$

$$[\Phi_0, h]^0 \equiv (1/x)\{\Phi_0' h'' + \Phi_0''[h' - (n^2/x)h]\}.$$

Since the stresses and displacements are bounded and single-valued at $x = 0$, we conclude from (2.1), (2.2), (3.1) and (3.4) that

$$y_n(0) = z_n(0) = 0, \quad n = 1, 2, \cdots. \tag{3.6b}$$

These equations also imply that $y_n'(0) = z_n'(0) = 0$, $n = 2, 3, \cdots$, and $y_1'(0)$ and $z_1'(0)$ are arbitrary. However, we shall not explicitly need to use these conditions on the derivatives. Thus the wrinkling loads $P = P_0(\lambda, n)$ are determined by solving the eigenvalue problems (3.5) and (3.6).

4. The numerical determination of the wrinkling loads. We numerically determined eigenvalues of (3.5) and (3.6) by a finite difference method essentially equivalent to the method used by Huang [3] in a related study of spherical caps. Thus we define new dependent variables $u_n(x)$ and $v_n(x)$ by $u_n = y_n''$ and $v_n = z_n''$. Then (3.5) is equivalent to the following system of four second-order equations:

$$\begin{aligned} M_n u + Q_n y + (1/x)\{W_0' v + W_0''[z' - (n^2/x)z]\} &= 0, \\ M_n v + Q_n z - (1/x)\{W_0' u + W_0''[y' - (n^2/x)y]\} & \\ - (1/x)\{F_0' v + F_0''[z' - (n^2/x)z]\} &= 0, \\ y'' = u, \qquad z'' = v, & \end{aligned} \tag{4.1}$$

* We can choose the coordinate system so as to remove a possible phase shift in θ.

for the four-component vector

$$\mathbf{s}(x) \equiv \begin{bmatrix} y(x) \\ z(x) \\ u(x) \\ v(x) \end{bmatrix}. \tag{4.2}$$

We have omitted the subscript n on s and its components in (4.1) to simplify the notation. The operators M_n and Q_n are defined by

$$\begin{aligned} M_n h &\equiv h'' + \frac{2}{x} h' - \frac{(1 + 2n^2)}{x^2} h, \\ Q_n h &\equiv \frac{(1 + 2n^2)}{x^3} h' + \frac{n^2(n^2 - 4)}{x^4} h. \end{aligned} \tag{4.3}$$

To obtain numerical solutions of (4.1) and (3.6), we divide the unit interval into N equal intervals by the net points,

$$x_j = j\delta, \quad j = 0, 1, \cdots, N, \quad \text{where} \quad \delta \equiv 1/N. \tag{4.4}$$

Furthermore, we define the exterior net point x_{N+1} by $x_{N+1} \equiv (N + 1)\delta$. At each point $x_1, x_2, \cdots, x_N$, we approximate the derivatives in (4.1) by centered difference quotients. We also use central difference approximations for the derivatives in (3.6a). This yields the following system of algebraic equations for the mesh vectors $\mathbf{S}_j$:

$$A_j\mathbf{S}_{j+1} + B_j\mathbf{S}_j + C_j\mathbf{S}_{j-1} = 0, \quad j = 1, 2, \cdots, N \tag{4.5}$$

$$D\mathbf{S}_{N+1} + E\mathbf{S}_N - D\mathbf{S}_{N-1} = 0. \tag{4.6}$$

The four-component mesh vectors $\mathbf{S}_j$ are assumed to converge to $\mathbf{s}(x_j)$ as $\delta \to 0$ for $j = 0, 1, \cdots, N$. The 4×4 matrices A_j, B_j, C_j, $j = 1, 2, \cdots, N$, and D and E are defined in Appendix A.

We conclude from the definition of C_1 in Appendix A and (3.6b) that

$$C_1\mathbf{S}_0 = 0 \tag{4.7}$$

for arbitrary values of $u(0)$ and $v(0)$. Thus $\mathbf{S}_0$ is eliminated from (4.5). We eliminate $\mathbf{S}_{N+1}$ from (4.5) by using (4.6). The system (4.5) and (4.6) is then reduced to

$$Q\mathbf{S} = 0. \tag{4.8}$$

Here Q is the block tridiagonal matrix defined by

$$Q = [C_i, B_i, A_i] \equiv \begin{bmatrix} B_1 & A_1 & 0 & 0 & 0 & \cdots & 0 \\ C_2 & B_2 & A_2 & 0 & 0 & \cdots & 0 \\ 0 & C_3 & B_3 & A_3 & 0 & \cdots & 0 \\ \vdots & & \ddots & \ddots & \ddots & & \vdots \\ \vdots & & & \ddots & \ddots & \ddots & 0 \\ & & & 0 & C_{N-1} & B_{N-1} & A_{N-1} \\ 0 & \cdots & \cdots & \cdots & 0 & C_N^0 & B_N^0 \end{bmatrix} \tag{4.9}$$

and B_N^0 and C_N^0 are defined by

$$B_N^0 \equiv -DA_N^{-1}B_N + E, \qquad C_N^0 \equiv -D(A_N^{-1}C_N + I). \tag{4.10}$$

I is the 4×4 unit matrix. The composite vector $\mathbf{S}$ has the components $\mathbf{S}_1, \mathbf{S}_2, \cdots, \mathbf{S}_N$.

The values of P for which the algebraic system (4.8) has nontrivial solutions are approximations to the wrinkling loads $P_0(\lambda, n)$. To determine these values, we factor Q into the product of a lower block triangular matrix L and an upper block triangular matrix U, i.e.

$$Q = LU. \tag{4.11}$$

Using the notation of (4.9), the block triangular matrices are given by

$$L \equiv [l_i, I, 0], \qquad U \equiv [0, U_i, A_i]. \tag{4.12}$$

The 4×4 scalar matrices l_j and U_j are defined by

$$\begin{aligned} l_j &\equiv C_j U_{j-1}^{-1}, \\ U_j &\equiv B_j + C_j Q_{j-1}, \qquad j = 2, 3, \cdots, N-1, \\ U_1 &\equiv B_1, \\ l_N &\equiv C_N^0 U_{N-1}^{-1}, \\ U_N &\equiv B_N^0 + C_N^0 Q_{N-1}, \end{aligned} \tag{4.13a}$$

and the matrices Q_j are recursively defined by

$$Q_0 = 0, \qquad Q_j = -U_j^{-1}A_j, \quad j = 1, 2, \cdots, N-1. \tag{4.13b}$$

Therefore the factoring (4.11) is possible if and only if $U_1, U_2, \cdots, U_{N-1}$ are non-singular.

We assume that the factoring is possible. Since $\det L = 1$, (4.8) is equivalent to

$$U\mathbf{S} = 0. \tag{4.14}$$

Therefore (4.8) has nontrivial solutions if and only if $\det U = 0$. Since $U_1, U_2, \cdots, U_{N-1}$ are non-singular, the condition $\det U = 0$ is equivalent to

$$\phi(P, n, \lambda) \equiv \det U_N = 0. \tag{4.15}$$

The factoring was possible for all the calculations that were performed. Thus the wrinkling loads $P_0(\lambda, n)$ are approximated by the roots of (4.15).

Approximations for the roots of (4.15) were obtained by a chord method. That is, for each pair (λ, n) we evaluated ϕ for an increasing sequence of values of P and then located the sign changes in ϕ. The results are discussed in the next section.

To evaluate ϕ for each pair (λ, P), we require $W_0(x_j; P, \lambda)$ and $F_0(x_j; P, \lambda)$, $j = 0, 1, \cdots, N$ and their derivatives; see (4.13a), (4.10) and Appendix A. Approximations of them were obtained from an accurate numerical solution of Problem S using the shooting method described in [4]. The net used in the solution of Problem S contained the net (4.4).

When a root of (4.15) was determined, we obtained an eigenvector of (4.14) by first evaluating $\mathbf{S}_N$ as the normalized eigenvector of the 4×4 system

$$U_N\mathbf{S}_N = 0. \tag{4.16}$$

Then it follows from (4.12) and (4.14) that the remaining components of $\mathbf{S}$ are determined by solving the recursions

$$U_j\mathbf{S}_j = -A_j\mathbf{S}_{j+1}, \qquad j = N-1, N-2, \cdots, 1. \tag{4.17}$$

The subvectors $\mathbf{S}_1, \cdots, \mathbf{S}_{N-1}$ are uniquely determined in terms of $\mathbf{S}_N$ by (4.17) since the U_j, $j = 1, 2, \cdots, N-1$ are nonsingular.

Acceptable values of δ were determined from test calculations of P_0 for sequence of decreasing values of δ. We concluded that $\delta = .02$ was adequate for the accuracy we desired in most of the calculations.

5. The numerical results for the wrinkling loads. The roots of (4.15) were determined by first fixing λ and finding the roots of (4.15) for a sequence of values of n. Then λ was changed and the process was repeated. We determined only one root for each pair (λ, n), although other much larger roots may exist. Thus for each λ that we considered there were many roots, one for each value of n. In Table I we present the numerical approximations of $P_0(0, n)$ for the pure bending problem for several values of n.

TABLE I

Numerical wrinkling loads for the pure bending problem

n	14	13	15
$P_0(0, n)$	62,600	62,800	64,025

We denote the smallest positive wrinkling load for fixed λ by $P_c(\lambda)$ and the corresponding value of n by $n_c(\lambda)$, i.e. $P_c(\lambda) = P_0(\lambda, n_c(\lambda))$. We refer to P_c as the critical wrinkling load. In Table II and Fig. 4 we summarize numerically-determined values of $P_c(\lambda)$ and $n_c(\lambda)$. For $\lambda \leq 100$, $P_c(\lambda)$ is essentially a linear function. It is approximated by

$$P_c = 62600 - 480\lambda, \quad -5 \leq \lambda \leq 100. \tag{5.1}$$

We observe that for $\lambda \geq 100$, n_c decreases as λ increases.

According to the mechanism described in Sec. 2, wrinkling is caused by the large circumferential compressive stresses adjacent to the edge of the plate in the symmetric state. This stress results from the combined effects of P and λ. Since small (large) values of λ create weak (strong) compressive strips, large (small) values of P are required to induce wrinkling. This explains the decrease of $P_c(\lambda)$ as λ increases in the range $-5 \leq \lambda \leq 100$.

At $\lambda = 110$, the plate wrinkles without lateral pressure. Thus $\lambda = 110$ is a secondary buckling load for the pure buckling problem. Other secondary buckling loads occur at $\lambda = 133$ and $\lambda = 152.5$. Presumably there are others for larger values of λ. We observe that for the pure buckling problem, $n_c(\lambda)$ increases with the magnitude of the secondary buckling loads.

The interval $100 \leq \lambda < 110$ presumably is a transition region in which the dominant cause of wrinkling shifts from P to λ. For $\lambda \geq 110$ the wrinkling is primarily a consequence of the compressive ring supplied by the edge thrust. We observe that except near the secondary buckling loads, $n_c(\lambda)$ generally increases.

TABLE II

Numerically-determined critical wrinkling loads

λ	n_c	P_c
−5	14	64,960
0	14	62,600
10	13	57,750
20	13	52,900
40	13	43,650
60	12	34,105
80	11	24,500
100	10	14,500
110	6	0
120	6	750
130	10	1,000
131	10	600
133	10	0
134	6	1,500
135	6	1,600
140	11	800
150	12	600
152.5	12	0
160	13	600
180	15	1,000
200	17	1,600

The numerical eigenfunctions evaluated from (4.16) and (4.17) are sketched in Figs. 5 for representative values of λ. The eigenfunctions essentially vanish near the center of the plate and then vary rapidly to a maximum near the edge. Thus when the plate wrinkles, the interior deforms nearly axisymmetrically. The unsymmetric deformation occurs near the edge, as we suggested in Sec. 2.

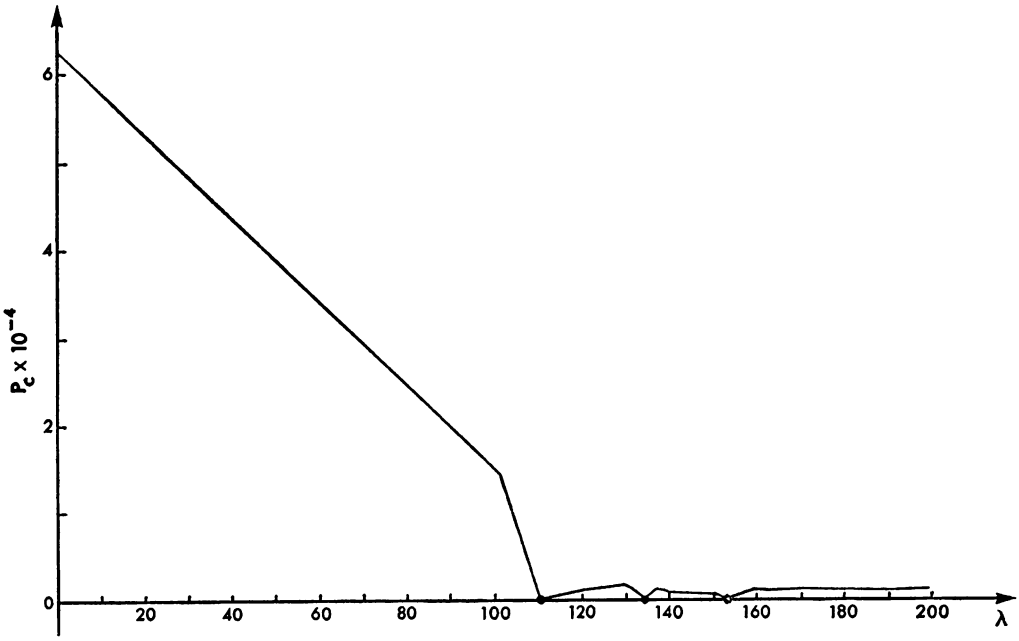

FIG. 4. The numerical results for the critical wrinkling load $P_c(\lambda)$.

The pure bending problem was studied previously by Panov and Feodosev [10] by a Galerkin procedure. Approximations were obtained in the form

$$W = (1 - x^2)^2(A + Bx^4 \cos n\theta) \tag{5.2}$$

for any integer $n \geq 2$. We denote the Panov and Feodosev wrinkling loads and critical wrinkling load by $P_0^*(n)$ and P_c^*. Their results are summarized in Table III (cf. Table I). Since $P_c^* = P_0^*(2) = 0$, Panov and Feodosev found that in addition to the axisymmetric state there is an unsymmetric state which branches from $P = 0$. However, this unsymmetric state is spurious because of Piechocki's [11] uniqueness theorem. This theorem states that there is a unique solution of Problem B with $\lambda = 0$ for all sufficiently small P. Since we can establish the existence of a solution of Problem S with $\lambda = 0$ for all sufficiently small P using, for example, the analysis in [7], we conclude that an unsymmetric solution cannot branch from $P = 0$. Furthermore, we observe by comparing Tables I and III that Panov and Feodosev's wrinkling loads and corresponding wave numbers differ substantially from the present results. Thus, (5.2) may be too inaccurate to adequately describe the wrinkling of the plate.

6. The post-wrinkling behavior. We employ a formal perturbation expansion to obtain approximations of the solution of Problem B for P near the eigenvalues P_0 of (3.3). Thus we assume that w, f and P in (3.1) are analytic in ϵ for sufficiently small ϵ and that $P(\epsilon) \to P_0$ as $\epsilon \to 0$. That is, we seek solutions of Problem B in the form (3.1) with

$$w(x, \theta; P(\epsilon), \epsilon) = \sum_{m=0}^{\infty} w^{(m)}(x, \theta)\epsilon^m,$$

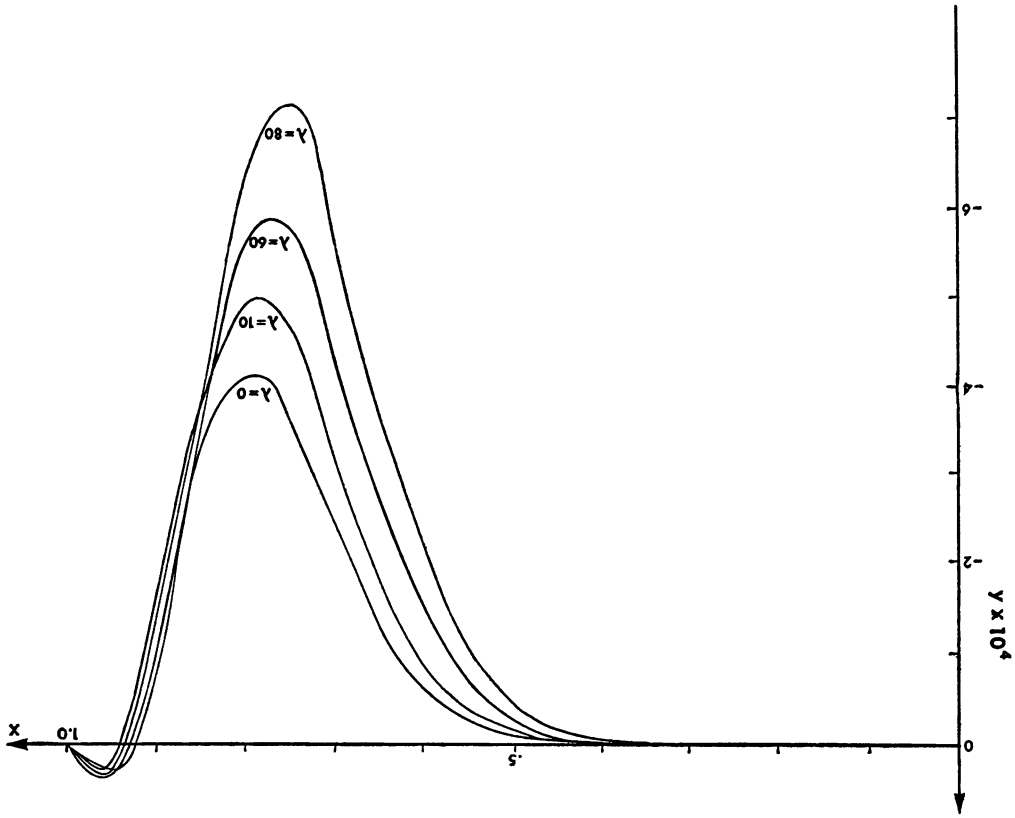

FIG. 5a. The y component of the numerically-determined and normalized eigenfunctions (wrinkling modes) at $P = P_c$ for a sequence of values of λ. The value of n for each λ is given in Table II.

$$f(x, \theta; P(\epsilon), \epsilon) = \sum_{m=0}^{\infty} f^{(m)}(x, \theta)\epsilon^m, \tag{6.1}$$

$$P(\epsilon) = \sum_{m=0}^{\infty} P_m \epsilon^m,$$

and we expand the solution $\{W_0(x; P(\epsilon)), F_0(x; P(\epsilon))\}$ of Problem S in a power series in ϵ. We define the parameter ϵ by

$$\epsilon^2 \equiv \iint [(W - W_0)^2 + (F - F_0)^2]\, dA = \epsilon^2 \iint (w^2 + f^2)\, dA \tag{6.2}$$

where the integrals are over the unit circle. Other definitions of ϵ can be used. The coefficients $w^{(m)}$, $f^{(m)}$ and P_m are determined by substituting (3.1), (6.1) and the expansions for W_0 and F_0 into (3.2) and (6.2). Then, by equating coefficients of the same powers of ϵ, we obtain a sequence of linear boundary-value problems and a sequence of normalizing conditions. For $m = 0$ we obtain the eigenvalue problem (3.2) and the normalizing condition

$$\iint [w^{(0)2} + f^{(0)2}]\, dA = 1. \tag{6.3}$$

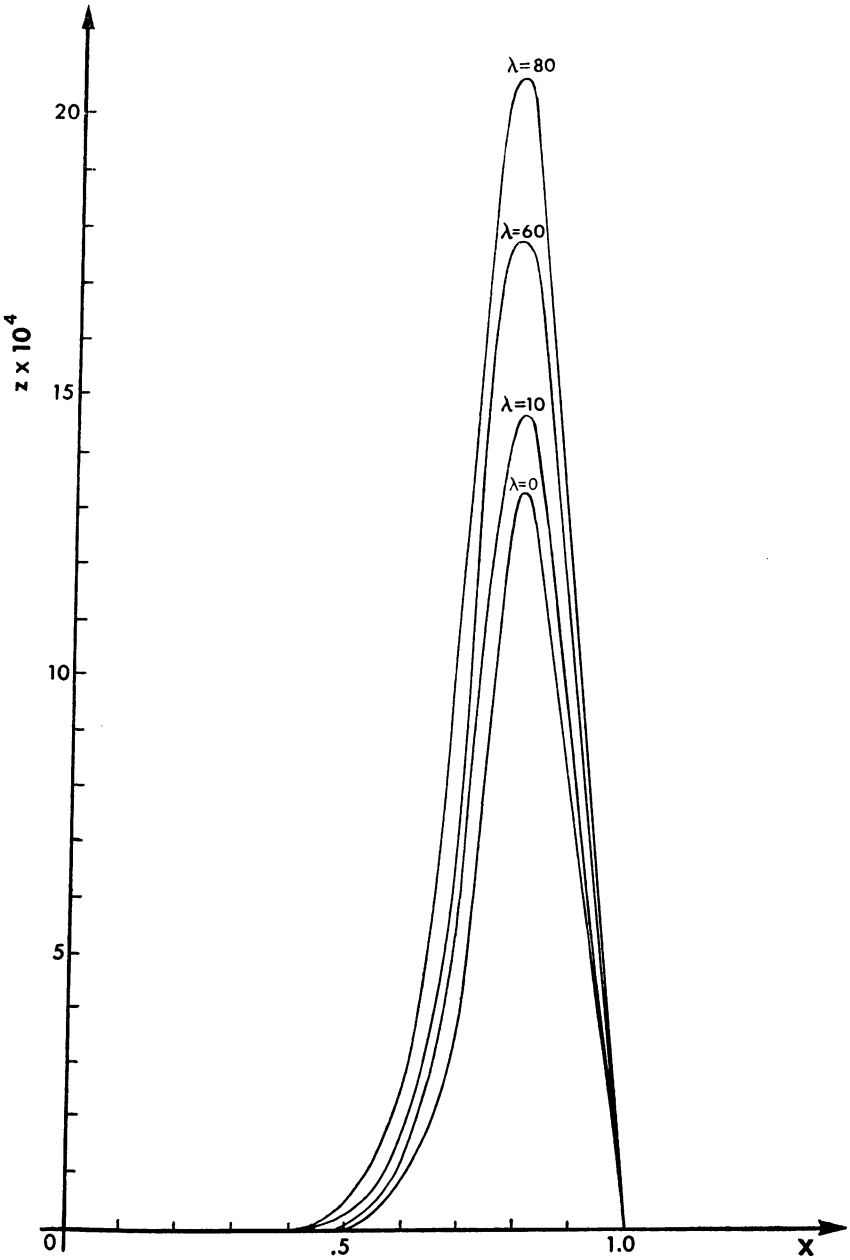

FIG. 5b. The z component of the numerically-determined eigenfunctions at $P = P_e$.

Thus $\{w^{(0)}, f^{(0)}\}$ is a normalized eigenfunction and P_0 is the eigenvalue. For $m > 0$ the boundary-value problems are inhomogeneous and the corresponding homogeneous problems have nontrivial solutions since they are the same as (3.2). The solvability conditions for the inhomogeneous problems then give P_m as integrals of $w^{(k)}$ and $f^{(k)}$ for $k < m$. The solutions of the linear boundary-value problems, which are required

TABLE III

Panov and Feodosev [10] *wrinkling loads* $P_0^*(n)$ *for the pure bending problem*

n	2	8	9	7	6	5
$P_0^*(n)$	0	25,415	26,142	27,333	34,010	50,849

to evaluate these integrals, were obtained by separating out the θ dependence. Then the resulting boundary-value problems were solved numerically by the shooting and the parallel shooting methods described in [4]. The parallel shooting method was required for some of the equations since their coefficients are large for the values of n that we considered. The amplitudes of the complementary solutions were determined from the appropriate normalizing conditions in (6.3).

In all cases that we studied, $P_1 \equiv 0$. In Table IV we give some representative numerical values of $P_2(\lambda)$ for the solutions branching from $P_c(\lambda)$. We observe that the numerically-determined values of P_2 are negative and small compared to P_c. To determine whether these values are numerically significant or whether they are approximations of $P_2 = 0$, we obtained P_2 for the sequence of finer meshes $\delta = 1/100$, $\delta = 1/200$ and $\delta = 1/400$ and representative values of λ. The corresponding values of P_2 changed only slightly. Hence in the following discussion we shall assume that $P_2 < 0$, as suggested by the numerical results. (If indeed $P_2 = 0$, then we must determine higher-order terms in (6.1) to study the branching process near P_c.)

For small ϵ we have, from (6.1),

$$P = P_c + P_2\epsilon^2 + 0(\epsilon^3). \tag{6.4}$$

We say that a solution branches down (up) from a wrinkling load P_0 if it exists near $P = P_0$ and $\epsilon = 0$, only for $P < P_0$ ($>P_0$). The branching is downward at the values of P_c that we studied since $P_2 < 0$. The potential energies of the unsymmetric states for $P < P_c$ were less than the potential energy for the symmetric state at $P = P_c$.

TABLE IV

The post-wrinkling numerical results for solutions branching from $P_c(\lambda)$

λ	P_c	$-P_2 \times 10^2$
0	62,600	4.08
10	57,750	5.74
20	52,900	7.85
40	43,650	16.18
60	34,105	39.95
80	24,500	68.02

To interpret the numerical results we consider a hypothetical experiment in which λ is held fixed and P is increased from zero. As P increases the plate is in an axisymmetric equilibrium state. Suppose for the present that the plate does not jump or is constrained from jumping from the axisymmetric state to another equilibrium state. By definition, no equilibrium states branch from the axisymmetric state for $P < P_c$. Since jumping is not permitted, the plate remains in the axisymmetric state until P reaches P_c. At $P = P_c$ it is possible for the plate to deform continuously from the axisymmetric to an unsymmetric state. However, the unsymmetric solution branches downward from P_c. Since we consider P as increasing through P_c, the smooth transition to the unsymmetric state at $P = P_c$ cannot occur. In general, if an unsymmetric solution branches up (down) a smooth transition from the symmetric to the unsymmetric state can occur only for P increasing (decreasing). We have calculated P_2 for the first one or two wrinkling loads above P_c for representative values of λ. In all cases we found that $P_2 < 0$. This does not preclude the possibility that $P_2 > 0$ for some sufficiently large wrinkling load. At these loads, the smooth transition to an unsymmetric state could occur.

We now permit discontinuous transitions from the symmetric to unsymmetric states, i.e. we allow jumping to occur. Then wrinkling may occur as P approaches P_c from below. In any real experiment the disturbances may be sufficiently large to trigger a jump from the axisymmetric state to an unsymmetric state. The plate need not jump to the solution branching down from P_c. It could jump to another unsymmetric state. The possibility of jumping depends on the initial disturbances and the number and proximity of unsymmetric solutions. However, the jumping is likely to occur for P just below P_c since there are unsymmetric states close to the symmetric state. If the potential energies of the wrinkled states near $P = P_c$ are less than the corresponding potential energy of the symmetric state then jumping might be "easier".

Thus the numerical results suggest that if wrinkling occurs at or near $P = P_c$ then it occurs by jumping. If wrinkling by a smooth transition from the symmetric state is possible, then it must occur at a wrinkling load $> P_c$.

Appendix A. The matrices of the difference equations. The sub-matrices of the algebraic equations (4.5) and (4.6) are defined by

$$A_j \equiv \delta^{-2}\begin{bmatrix} \dfrac{1+2n^2}{2j^3\,\delta^2} & \dfrac{W_0''(x_j)}{2j} & \dfrac{j+1}{j} & 0 \\ \dfrac{-W_0''(x_j)}{2j} & \left(\dfrac{1+2n^2}{2j^3h^2} - \dfrac{F_0''(x_j)}{2j}\right) & 0 & \dfrac{j+1}{j} \\ -1 & 0 & 0 & 0 \\ 0 & -1 & 0 & 0 \end{bmatrix},$$

$$B_j \equiv \delta^{-2}\begin{bmatrix} \dfrac{n^2(n^2-4)}{j^4\,\delta^2} & \dfrac{-n^2W_0''(x_j)}{j^2} & -\left(2+\dfrac{1+2n^2}{j^2}\right) & \dfrac{\delta W_0'(x_j)}{j} \\ \dfrac{n^2W_0''(x_j)}{j^2} & \dfrac{n^2}{j^2}\left(\dfrac{n^2-4}{j^2\,\delta^2}+F_0''(x_j)\right) & \dfrac{-\delta W_0'(x_j)}{j} & -\left[2+\dfrac{(1+2n^2)}{j^2}+\dfrac{\delta F_0'(x_j)}{j}\right] \\ 2 & 0 & \delta^2 & 0 \\ 0 & 2 & 0 & \delta^2 \end{bmatrix},$$

$$C_i \equiv \delta^2 \begin{bmatrix} \dfrac{-(1+2n^2)}{2j^3\,\delta^2} & \dfrac{-W_0''(x_j)}{2j} & \dfrac{j-1}{j} & 0 \\ \dfrac{W_0''(x_j)}{2j} & \left(\dfrac{1+2n^2}{-2j^3\,\delta^2} + \dfrac{F_0''(x_j)}{2j}\right) & 0 & \dfrac{j-1}{j} \\ -1 & 0 & 0 & 0 \\ 0 & -1 & 0 & 0 \end{bmatrix}, \quad j = 1, 2, \cdots, N-1,$$

$$D \equiv \frac{1}{2\delta} \begin{bmatrix} 0 & 0 & 0 & 0 \\ 0 & 0 & 0 & 0 \\ 1 & 0 & 0 & 0 \\ 0 & 1 & 0 & 0 \end{bmatrix}$$

$$E \equiv \begin{bmatrix} 1 & 0 & 0 & 0 \\ 0 & 1 & 0 & 0 \\ 0 & 0 & 0 & 0 \\ 0 & 0 & 0 & 0 \end{bmatrix}, \qquad A_N = C_N = -(2/\delta)D.$$

The matrix B_N is obtained by replacing the first two rows in B_i by zeros.

References

[1] T. von Kármán, *Festigkeitsprobleme in Maschinenbau*, Ency. Math. Wiss. **4**, 348–352, Teubner, Leipzig, 1910

[2] M. Yanowitch, *Non-linear buckling of circular plates*, Comm. Pure Appl. Math. **9**, 661–672 (1956)

[3] N. C. Huang, *Unsymmetrical buckling of thin shallow spherical shells*, J. Appl. Mech. **31**, 447–457 (1964)

[4] L. Bauer, E. L. Reiss and H. B. Keller, *Axisymmetric buckling of hollow spheres and hemispheres*, Comm. Pure Appl. Math. **23**, 529–568 (1970)

[5] K. O. Friedrichs and J. J. Stoker, *Buckling of the circular plate beyond the critical thrust*, J. Appl. Mech. **9**, A7-A14 (1942)

[6] N. F. Morozov, *Investigation of a circular symmetric compressible plate with a large boundary load*, Izv. Vyssh. Ucheb. Zav. **34**, 95–97 (1963)

[7] H. B. Keller and E. L. Reiss, *Iterative solutions for the non-linear bending of circular plates*, Comm. Pure Appl. Math. **11**, 273–292; *Non-linear bending and buckling of circular plates*, Proc. 3rd U. S. Nat. Cong. of Appl. Mech. 375–385 (1958)

[8] E. L. Reiss, *A uniqueness theorem for the non-linear axisymmetric bending of circular plates*, AIAA Jour. **1**, 2650–2652 (1963)

[9] T. von Kármán, E. E. Sechler and L. H. Donnell, *The strength of thin plates in compression*, Trans. A.S.M.E. **54**, APM 53–57 (1932)

[10] D. Panov and V. Feodosev, *Equilibrium and loss of stability of shallow shells with large deflections*, P.M.M. **12**, 389–406 (1948)

[11] W. Piechocki, *On the non-linear theory of thin elastic spherical shells*, Arch. Mech. Stos. **21**, 81–101 (1969)